Glideosomal GAP50 binders that inhibit invasion and restrict malaria parasite *in vitro* and *in vivo*

PRAKHAR AGRAWAL
International Centre for Genetic Engineering and Biotechnology
SUREKHA KUMARI
Institute of Himalayan Bioresource Technology
UPENDRA SHARMA
Institute of Himalayan Bioresource Technology
DINKAR SAHAL (dsahal@gmail.com)
International Centre for Genetic Engineering and Biotechnology

Research Article

Keywords: Malaria, Plasmodium, GAP50, Merozoite, invasion, Bedaquiline, Brilacidin, Hayatinine, Curine

Posted Date: December 17th, 2021

DOI: https://doi.org/10.21203/rs.3.rs-1099040/v2

Abstract

Malaria continues to be a killer disease even in the modern world. Vaccines and drugs have a lot to learn from the malaria parasite before they can be successful. Here, using a filter for glideosomal anchor protein *Pf*GAP50, we have explored a plethora of small molecules to shortlist eight GAP50 binders with promising antiplasmodial activity (IC_{50} < 3 μM) that are also highly selective. Of these, Hayatinin, Bedaquiline, MMV688271, Curine, and Brilacidin with *Pf*NDO $IC_{50} \leq 1$ μM were found to stall merozoites invasion by inhibiting IMC formation besides increasing ROS levels in trophozoites. Bedaquiline loaded healthy RBCs showed prophylactic ability to prevent intraerythrocytic development of malaria parasite. Synergistic activities with ΣFIC values as low as 0.22 (Curine and Artemisinin) or 0.37 (Bedaquiline and Artemisinin) augur well for the development of drug combinations to combat malaria effectively. Interestingly, orally delivered Bedaquiline (50 mg/Kg b. wt.) showed substantial suppression of parasitemia in the mouse model of malaria.

Significance Of The Work

Our study offers a new set of drug-like molecules targeting the invasion machinery and asexual stages of malaria parasite that may have good prospects against other parasitic apicomplexans as well. These molecules can be starting points for future optimization towards the design of novel antimalarials.

Introduction

Notwithstanding intense efforts to discover drugs and vaccines and attempts to combat it through vector control, malaria continues to be a deadly curse in Africa, Asia, and South America. With the emergence of artemisinin-resistant parasite strains and the inability of Artemisinin Combination Therapies (ACT) to clear them, there is a need to identify and aim antimalarials at novel targets with new mechanisms of action. In humans, the mosquito vector-borne malaria parasite traverses through different developmental stages, first in the liver and then in the blood. Most importantly, exponential parasite proliferation accompanied by the malaria pathology is initiated following the invasion of RBCs by merozoites. Hence malaria can be stymied if invasion by blood-stage malaria parasite is blocked.

The invasive molecular machinery of the malaria parasite is fine-tuned for the initial attachment of merozoites, followed by the formation of a tight junction between the invading merozoite and the red blood cell membrane. However, the force required to penetrate the host RBCs is generated by the parasite's multiprotein glideosomal machinery consisting of GAP50, GAP45, MTIP, and MyoA. Of these, GAP50 plays a pivotal role by acting first as a scaffolding protein and next by anchoring the glideosomal complex to the inner membrane leading to the positioning of the complex in the space between the plasma membrane and the inner membrane[1,2]. Among the proteins of this complex, actin-myosin and myosin A/MTIP complex have been explored as drug targets, and a few natural products such as Latrunculins, Cytochalasins and synthetic pyrazole-based urea peptides such as C416 have been shown to prevent RBC invasion by blocking actin polymerization and MTIP/MyoA association[3,4].

In this study, we have chosen to explore small molecules of diverse chemical classes to target the hitherto neglected, highly conserved *Pf*GAP50 anchor protein of the glideosomal machinery. Further, *Pf*GAP50 has been found also to be a key member of *Pf*Phil1, a newly identified multiprotein complex located close to glideosomal complex within the inner membrane complex and to be crucially involved in invasion[5]. We surmised that small molecules targeting *Pf*GAP50 might disrupt the delicate organization of the glideosomal complex and the Phil1 complex and prevent invasion, thereby limiting the exponential rise in %Parasitemia. To achieve our goal, we first screened about a thousand different compounds coming from azepino quinolines, MMV pathogen, and pandemic boxes and medicinal plant-derived natural products against *Pf*GAP50 using Schrödinger drug discovery suite. Further, we used recombinantly expressed, and affinity-purified *Pf*GAP50 to study the binding of this protein to our library of small molecules using surface plasmon resonance (SPR). Our screening has led to the identification of five potent antiplasmodial lead molecules endowed with high selectivity and low resistance indices that are gifted with the ability to prevent the nefarious act of invasion by the malaria parasite. In the present work, these five anti-invasion molecules with a potential to develop into new antimalarials have been studied for the first time against malaria.

Results

A total of 951 different compounds from diverse chemical libraries [pathogen box (400), pandemic box (400), Azepino quinolines (140), and specialized secondary metabolites purified from *C. pareira* (11)] were screened for their *in silico* binding to *Pf*GAP50 by via (a) Schrödinger drug discovery suite, **(b)** differential scanning fluorimetry (DSF) and **(c)** SPR. As shown **(Fig-1a),** employing different filters at successive stages, we shortlisted 345 (after *in silico* Extra Precision (XP) mode docking and DSF), 39 (after *in vitro* antiplasmodial assay), 8 (after consideration of both anti *Pf* IC_{50} and selectivity indices) and 3 (after checking the disruption of inner membrane complex and invasion). Upon analysis of results, it was interesting to know that of the pathogen and pandemic box molecules shortlisted as *Pf*GAP50 binders, 20 were those that had been pre-approved by the FDA for the treatment of fungal, bacterial, and viral infections.

For molecules selected from MMV, the *Pf*GAP50 KD values (in parentheses, μM) observed were Mefloquine (40), Suramin (28.6), Bitertanol (0.333), Letermovir (19.2), Everolimus (0.257), Deferasirox (4.93), Valdecoxib (9.63), Ketoconazole (16.5), Ezetimibe (1.16), LED209 (2.62), Birinapant (12.4), Mgb Bp3 (14.8), Alexidine (27.0), Tipifarnib (52.2), Eberconazole (75.9), Ozanimod (76.5), Pentamidine (12.7), Rifampicin (0.116), Bedaquiline (9.27) and Brilacidin (2.81). The other MMV molecules identified as *Pf*GAP50 binders are pending approval as drugs **(SI_2)**. Although Mefloquine, Suramin, Rifampicin, and Pentamidine were identified as binders to *Pf*GAP50, their discontinued use against malaria[6–8] led us not to subject them for detailed *in vitro* stage-specific and IMC inhibition assays. Among 11 molecules from *C. pareira* **(SI-1_Fig 2)**, Hayatinine, Curine, and Magnocurarine were identified as *Pf*GAP50 binders with KD below 100 μM **(SI-1_Table-2)**.

In vitro antiplasmodial potency and mammalian cell cytotoxicity

Our next step for shortlisting molecules was screening for potencies of molecules for their antiplasmodial IC_{50}s against chloroquine-sensitive Pf3D7, chloroquine-resistant PfINDO, and artemisinin-resistant PfCam 3.1^{R539T} strains. We shortlisted the best top eight molecules on the basis of IC_{50s} and selectivity indices **(Fig-1b; Table 1)**. It is noteworthy that among shortlisted molecules, Bedaquiline aka MMV689758 (anti-tuberculosis molecule), MMV1634402 aka Brilacidin (a mimic of host defense peptide defensin), MMV688271 MMV642550 and Hayatinine showed $IC_{50s} \leq 1.5$ µM against all the three strains of Plasmodium. USINB4-124-8 and Hayatinine were found to be more active against PfCam 3.1^{R539T} (IC_{50} 6.7 nM and 80 nM, respectively) than against PfINDO strain (IC_{50} 2.42 µM and 0.41 µM, respectively). On the other hand, MMV1782353 and Curine, which showed RIs < 1 ($RI_{INDO/3D7}$ 0.64 and 0.34, respectively), exhibited RI >1 against PfCam 3.1^{R539T} ($RI_{1240/3D7}$ 21.25 and 1.91, respectively).

Table 1 is in the supplementary files section.

Inhibition of asexual stages of *P. falciparum*

In its replicative phase, the malaria parasite traverses through diverse cell cycle stages like the ring (R), trophozoite (T), and the Schizont (S). These three stages have morphologically identifiable sub-stages like early (E), intermediate and late (L). During these transitions, there are distinct changes in chromatin remodelling, transcriptome, and proteome of the malaria parasite, making some targets fade away and some new targets emerge[9]. Hence it is not surprising to expect that IC_{50} determined against different stages of the malaria parasite can be quite different. In a bid to explore the differential vulnerability of cell cycle stages of the malaria parasite to our lead antiplasmodial molecules, we subjected different stages of the parasite to each lead molecule at different concentrations. As shown (**Table-1)**, there were marked differences in the observed IC_{50s} against different stages. Taking ER to LR, ET to LT, ES to LS, and LS to ER stages into consideration, the ratio of the highest to the lowest IC_{50s} obtained ranged from 54.3 µM (USINB4-124-8) to 0.58 µM (MMV688271). As a specific example, USINB4-124-8 showed a much higher IC_{50} (µM) (38.12) against trophozoites and schizonts (54.32) than against rings (7.2). In contrast, MMV1782353 and MMV642550 showed good activity (IC_{50} < 5 µM) against early and late schizonts while showing less potency (IC_{50} > 8 µM) against rings (**Table-2**). It is noteworthy that despite great structural resemblance **(Fig-1b)**, Hayatinine (608.7 Da) showed a marked preference to prevent LS to ER transition whereas the preference for Curine (594 Da) was ES to LS along with ET to LT transitions.

Kill kinetics of test molecules

To understand the time kinetics of action by these test molecules on development, egression, and invasion events of *P. falciparum*, we treated *Pf*NDO rings and schizonts for variable times. Briefly, rings (6 - 12 h p.i), and schizonts (32 - 36 h p.i), were treated with test molecules (at IC_{50} and 2x IC_{50}) for variable times (D^+) as indicated (**Fig-2a)**, followed by culture in test molecule free medium (D^-) for a total ($D^+ + D^-$) time of 96 h. MMV1782353 (0.4 µM), MMV642550 (1.2 µM) and MMV1634402 (0.67 µM) were found to reduce %P in cultures grown under D^+16 h and D^- 80 h conditions to half the %P of the control. In contrast, MMV6888271 (0.25 µM) and Hayatinine (0.41 µM) caused 90 % reduction in %P following 12 h D^+ 84 h D^- treatments **(SI-1_Fig-9)**. USINB4-124-8 (2.42 µM), on the other hand, did not cause any reduction in %P by 12 h D^+ - 84 h D^- treatment. 24 h D^+ - 72 h D^- treatment did show a reduction of 25 % but drastic reduction up to 95 % was seen only when D^+ treatment was for 36h. Bedaquiline (1.09 µM), while not hindering stage progression, was found to significantly inhibit invasion of fresh RBCs by merozoites **(SI-1_Fig-9)**.

Hayatinine and USINB4-124-8 decreased %P to half of the control in 16 h D^+ treatment of schizonts with microscopic images showing late-stage 46 h schizonts and merozoites in treated cultures vs fully formed rings in control cultures **(SI-1_Fig-10)**. Curine and MMV 642550 killed 90 % of schizonts following 8 h D^+ and the surviving parasites revealed non invasive merozoites (Curine) and pyknotic schizonts (MMV642550) vs rings in case of control **(SI-1_Fig-10)**. MMV1634402 and MMV1782353 showed schizontocidal effects after 4 h and 8 h D^+ treatments, respectively, with pyknotic schizonts seen after 12 h treatment. MMV688271 reduced %P to half of the control in 12 h D^+ treatment with surviving parasites seen invading and forming rings **(SI-1_Fig-10)**. A reduction of %P to basal level at 8 h D^+ treatment and pyknotic schizonts at 16 h D^+ treatment, suggested the schizontocidal action of Bedaquiline **(SI-1_Fig-10).**

Monitoring growth of malaria parasite in healthy RBCs “preloaded” with test molecules

Test molecules retained inside RBCs can prevent the growth and maturation of the parasite. However, entrapment of test molecules by healthy RBCs is hitherto not a very well explored prophylactic strategy. In this experiment, healthy RBCs preincubated with different test molecules for 72 h and thereafter given centrifugal washes to remove test molecules from the medium, were exposed to mature “about to egress” schizonts. Parasitemia was monitored after 96 h. Control, Curine, Hayatinine, MMV642550, and USINB4-124-8 treated RBCs showed 100 % growth **(Fig-2b)**. On the other hand, MMV642550, MMV1634402, and

MMV688271 treated RBCs showed only 50 % growth of control indicating a decrease in growth and maturation rate of the parasite. Interestingly Bedaquiline loaded RBCs, showed necrotic trophozoites with % growth < 5 %. It appears that Curine, Hayatinine, MMV642550, and USINB4-124-8 are either not taken up or easily washed off and are not retained by healthy RBCs. On the other hand, MMV642550, MMV1634402, and MMV688271 appear to be retained partially, which causes partial retardation in parasite growth. In a prophylactic role, Bedaquiline appeared to be the best in being retained at concentrations that kill the parasite **(Fig-2b)**.

Effect of lead molecules on the rupture of schizonts and invasion by merozoites

Molecules with IC_{50} < 10 µM that were preventing egress or invasion during LS à ER transition were studied to examine inhibitions of egress from schizonts and invasion by merozoites into RBCs. In the presence of MMV1782353/ MMV642550, schizont maturation was found to be stalled but once these molecules were removed schizonts were able to rupture and release merozoites. However, the released merozoites were unable to invade, leading to a sharp decrease in %P with respect to -ve control **(Fig-2c)**. In the case of Hayatinine, and MMV1634402), 8 h treatment led to arrest at 46 to 48 h p.i schizonts with few merozoites stuck to the RBC membrane. Curine allowed schizont egress, but the level of invasion was significantly reduced. Both Bedaquiline and MMV688271 showed schizontocidal activity on mature about to rupture schizonts **(Fig-2c)**.

Effect of test molecules on ROS levels

Molecules showing IC_{50} (LRàT) < 10 µM, were taken at 2 x IC_{50} to assess their effects on ROS levels. Bedaquiline and MMV688271 were found to elevate ROS similar to H_2O_2 (100 µM) while MMV642550/MMV1634402 showed ROS levels similar to ART (700 nM). Further, in all samples, ROS levels were found to be quite similar at both 8 h and 12 h, suggesting 8 h treatment is sufficient to have maximum ROS levels. Although the parasite is adept in regulating ROS via the formation of hemozoin, Glutathione, and Catalase, the large excess production stimulated by the small molecules could overwhelm the parasite's ROS homeostasis, leading to its death. Among the seven molecules selected, only two molecules viz. Hayatinine and Curine showed only moderate elevation in ROS **(Fig-2d)**. This may be due to the combined effects of ROS stimulating and ROS scavenging[10] activities of these two molecules.

Putative antiplasmodial targets of Bedaquiline, Hayatinine, MMV1634402, MMV688271, and Curine

To find if there may be alternate targets other than GAP50 for the promising molecules studied by us, we performed cross-docking against 68 different malaria proteins, involved in different metabolic pathways of *Plasmodium*. Each lead molecule was docked into the active sites of selected proteins, and the scores for docking and dG binding were computed. Out of the 68 proteins studied (SI-Table 2), the number of the protein-ligand complexes with negative values for dG binding score were 63 (MMV688271), 47 (Bedaquiline), 18 (MMV1634402), 31 (Hayatinine), and 42 (Curine) **(SI-1_Table-9)**. Thirteen different proteins showed binding to all the five lead molecules **(Fig-2e)**.

IMC formation and invasion inhibition using Phil1 marker

Since *Pf*GAP50 is involved in the formation of IMC during schizogony[11] and anchors key proteins involved in invasion[12], we checked whether our lead GAP50 binder molecules could perturb IMC formation and invasion by merozoites. Indeed, two of the major inner membrane multiprotein complexes viz. Glideosomal complex[13] and Phil1 complex[14] play a key role in invasion. Interestingly pull-down experiments have demonstrated the presence of GAP50 in both these complexes[2,5,11]. We hypothesized that if IMC formation is disrupted, then the regular arrangement of Phil1 seen in control cells will not be seen in parasites with disrupted protein complexes. Our results showed that untreated control parasites showed distinct punctate green fluorescence marks on the periphery of schizont, indicating proper organization of Phil1 with GAP50 in IMC, and such parasites were highly invasive **(Fig-3, left panel, row A)**. However,in Bedaquiline, Hayatinine, and MMV1634402 treatment groups, an irregular distorted, depleted pattern of Phil1 fluorescence around developing merozoites was seen, suggesting a defect in IMC formation. In all instances where IMC formation was found to be distorted **(Fig 3, left panel, rows C, D, and F)**, we noticed a blockade of invasion as well **(Fig 3, right panel, rows C, D, and F)**. However, MMV688271 and Curine, which did not show any effect on IMC formation, nevertheless caused inhibition of invasion **(Fig-3)**.

In silico stabilities of complexes of *Pf*GAP50 with Bedaquiline, Hayatinine, MMV688271, Curine, and MMV1634402

Studying the finer nuances of the mode of binding of small molecule ligands to the target proteins of interest can facilitate the development of structure-based novel therapeutics. Towards this goal,

Bedaquiline and MMV688271 (pathogen box), Hayatinine and Curine (*Cissampelos pareira*), and MMV1634402 (pandemic box) were shortlisted based on the *in silico* screening followed by MD simulation to assess the dynamic stability of their intermolecular interactions with amino acid residues constituting the respective binding pockets in *Pf*GAP50 **(Fig-4)**.

Bedaquiline interaction was found to be primarily through hydrophobic interactions (W35, I69, H256, M278), hydrogen bonding (G65), and water bridge (N221), as seen through MD simulation **(Fig-4a)**. These interactions were found to be maintained over 30 % of 100 ns simulation time and appeared to help in stabilizing the binding of Bedaquiline with GAP50, resulting in -36.9 kcal/mol binding energy. The sensorgram profile obtained using one-on-one interaction with GAP50 suggested incomplete dissociation with a binding affinity (KD) 9.27 µM. Curine, that shares structural similarity with Hayatinine, was also found to bind to GAP50, but at a completely different site from that of Hayatinine **(SI-1_Fig-11)**. Residues interacting with Curine via hydrogen bonds, hydrophobic interactions, and water bridges were with Y96, L134, D135, D137, A138, V350, and E351 **(Fig-4b)**. On the other hand, Hayatinine was found to interact with G119, Q120, E133, M146, P147 and H152. The Hydrogen bonds, hydrophobic bonds, and water bridges with backbone and side chains of these amino acid residues persisting for more than 30 % of simulation time seem to prevent surface binder Hayatinine from moving out of its binding site. Interactions of MMV688271 **(Fig-4d)** with GAP50 were found to be stabilized through Hydrogen bonds (E123, H152, F344, L347, P348), water bridges (E123, H152, F344, L347), and hydrophobic interactions (H152, F344, L347, V350). MMV1634402 (Brilacidin) binding with GAP50 was found to be majorly driven by water bridges mediated via side chains and the backbone of N127, E129, N148, D201, I322, N349, E351, and L352 between ligand and protein which were further strengthened by Hydrogen bond interactions involving E129, E351, and L352. Amongst these interactions, the ones with E129 and E351 were maintained for > 50 % of 100 ns simulation time **(Fig-4e)**. A large number (sixteen) of water bridges between Brilacidin and GAP50, may have contributed to the lowest – dG of binding -64.82 kcal/mol, with a KD 2.81 µM.

In vitro effects of the combination of lead molecules with antimalarial drugs on ART resistant *P. falciparum*

Drug combinations help in the assessment of synergistic, additive, or antagonistic activities. This, in turn, helps in the selection of combinations that retard the development of resistance, reduce toxicity, and increase the efficacy of the drugs used. Herein, we tested our lead molecules (Hayatinine, Bedaquiline, MMV688271, Curine, and MMV1634402) in combination with standard antimalarial drugs (Mefloquine, Pyrimethamine, and ART) for their activity against intraerythrocytic development of ART resistant *P. falciparum*. In different test molecule and antimalarial drug combinations, strong synergy ($\sum$FIC < 1) was observed at a 1:4 molar ratio **(Table-2)**. These results show the importance of our lead molecules in

providing synergistic combinations for effective antimalarial therapy with a reduced probability of drug resistance.

Table 2 is in the supplementary files section.

In vivo toxicity and antimalarial study of Bedaquiline, and USINB4-124-8

USINB4-124-8 at 100 mg/kg b.wt did not show any signs of acute toxicity **(SI-1_Table-10)** and till day 16 mice were healthy with respect to control mice. Bedaquiline acute toxicity was not carried out as this molecule is already FDA approved for tuberculosis treatment. Treatment of P. berghei ANKA infected mice with vehicle solution (-ve control) led to the progressive increase in %Parasitemia with a median survival of 19 days and death of all 7 mice by day 22. These mice exhibited increased fluctuations in body temperature and a decrease in mean body weight with the progression of the disease. Interestingly, Bedaquiline (50 mg/kg b. wt.) resulted in the complete suppression of %Parasitemia by day 19, reduced fluctuations in temperature and body weight as compared to -ve control, and survival of three out of seven mice till 34 days **(Fig-5).** On the other hand, USINB4-124-8 (100 mg/kg b. wt.) showed no difference from -ve control in terms of survival, % rise in parasitemia, fluctuation in body weight, and temperature **(Fig-5)**.

Discussion

Control measures against the vector Anopheles mosquito and extensive use of artemisinin-based combination therapy (ACT) against the parasite have resulted in a marked decrease in malaria cases in the last decade[15]. However, the surge in malaria cases in developing Asian countries which have reported resistance to CQ, sulfadoxine-pyrimethamine, ACT, and other antimalarial combinations, demands new antimalarials against new targets to combat the threat of drug-resistant strains. An emerging strategy to kill *Plasmodium* is to target its Achilles' heel, viz invasion by sporozoites into hepatocytes, merozoites into erythrocytes, and ookinetes into mosquito gut wall. As many proteins of the merozoites bear similarity with proteins found in sporozoites and gametocytes[12,16], a small molecule preventing invasion by binding to a common target could block entry of malaria parasite into the safe milieu of different cells in man and mosquito. This could enable the immune system to kill the "out of cell" malaria parasite and not allow it to create havoc by the exponential rise in its numbers upon successful invasion into a cell. Once dead, resistance is not possible either. Thus, invasion into the host cell is the malaria parasite's greatest strategy to escape from the host immune responses because the immune system fails to be provoked into action by an intracellular parasite. We aimed to block invasion so as not to give the

parasite a chance for the exponential rise in %Parasitemia that malaria parasite ensures from within the safe confines of the host cell. Despite its vital importance to the parasite, only the major surface proteins of merozoite have been targeted for both vaccine and drug development while the highly conserved glideosomal proteins have remained largely neglected[17]. These motor proteins are involved in the meticulously organized development of the inner membrane complex that includes the IMC resident multiprotein complexes that are known to facilitate the highly efficient and extremely fast process of invasion by merozoites, sporozoites, and ookinetes. Among these proteins, glideosome associated protein 50 aka GAP50 is highly conserved in apicomplexan parasites and acts as an anchor for other motor proteins. Further GAP50 bears low homology to human protein homologs[18] which makes it a suitable target for drugs. The presence of conserved regions on the surface of GAP50[19], zygote motility inhibition by anti-GAP50 antibodies[20], and the ability of GAP50 to bind human complement factor H[21] suggest that this protein is of vital importance to the parasite. Hence GAP50 is well suited for designing the next generation of novel drugs against malaria.

In the absence of known inhibitors against this protein, our study has focussed on compounds belonging to diverse chemical classes for screening using *in silico* molecular docking and DSF with *Pf*GAP50 as the target. These two tools helped us in hit enrichment in a high throughput manner and narrowed down compounds for *in vitro* SPR and *in vitro* antiplasmodial activity. Even as the structural homology between GAP50 and hPAP (human purple acid phosphatases) is only 30%[19], we selected only those compounds which showed Selectivity Indices > 100 against HUH 7 and HEK293 human cell lines. This criterion helped to eliminate all those compounds that might be toxic by binding with hPAP or any other protein targets in the host. Since GAP50 is expressed in the late trophozoite and schizont stages (30 - 35 h p.i) of *Plasmodium* and is involved in IMC formation[11], we checked whether the inhibitors identified by us were able to prevent successful schizogony and egress of merozoites. In this attempt, we found some GAP50 binders to be schizontocidal. This inhibitory activity was further verified by setting up a 57 h stage-specific assay. This assay revealed that Hayatinine, Curine, USINB4-124-8, MMV688271, MMV1634402, MMV642550, and MMV1782353 were most active against trophozoites and schizonts which represent the mature replicative stages of *Plasmodium*. Bedaquiline, on the other hand, spared these mature stages and showed the highest activity against the step of invasion by merozoites. Moreover, most of these GAP50 binder molecules caused elevation of ROS levels that were at par with the levels elicited by the endoperoxide harboring Artemisinin's. High ROS levels induced by these molecules can overwhelm the ROS handling mechanisms of parasites leading to their death by oxidative damage. Our results suggest a possibility for protein targets other than GAP50 in the malaria proteome, which can, upon binding to the compounds studied by us, cause the death of the mature stages.

Our results on invasion inhibition showed Bedaquiline, Hayatinine, Curine, MMV688271, and MMV1634402 as potent inhibitors with % inhibition around 90%. Further, to find if the invasion was inhibited due to disruption of IMC and the GAP50 containing complexes therein, we did immunofluorescence-based confocal microscopy to study IMC formation using Phil1(a member of the Phil1 complex present in IMC) as an IMC marker. In independent experiments, the same compounds were

also tested for their ability to inhibit invasion. Our results indicated that Bedaquiline, MMV1634402, and Hayatinine, which prevented IMC formation, also caused invasion inhibition. On the other hand, the schizontocidal compounds Curine and MMV688271, which did not perturb IMC formation, did not inhibit invasion and may have preferential binding with proteins other than GAP50 involved in schizogony.

Data on the *in silico* binding of our lead molecules, i.e. MMV688271, Hayatinine, Curine, Bedaquiline, and MMV1634402 with GAP50 has shed light on the binding site residues, which can help in the optimization of these inhibitors to increase their potency and selectivity. Interestingly while Hayatinine and MMV688271 binding sites were found to consist predominantly of non-polar residues, the sites that recognized Bedaquiline and MMV1634402 were rich in polar residues. In contrast, the MMV688271 binding site contained an equal proportion of polar and non-polar residues. The involvement of water molecules in stabilizing Hayatinine, Curine, MMV688271, and MMV1634402 binding in their respective grooves shows the importance of these water bridges present in these regions. It is tempting to hypothesize that binding by the above-mentioned lead compounds may perturb the protein-protein interactions that are the hallmarks of the multiprotein complexes found in the IMC.

In a bid to explore what proteins other than GAP50 may bind to these lead compounds, we have found that these molecules may have thirteen different alternate protein targets besides GAP50. The binding of our lead compounds to one or more of these targets may well be the explanation for their multi-stage activity. Coupled with over hundred-fold selectivity, the presence of multi targets in malaria proteome could be a plus point for these compounds since multi-targeting drugs could have low chances of losing efficacy due to the development of resistance[22].

The longer half-life of small molecules *in vivo* is usually associated with their association with serum proteins or active uptake in cells from where they are released in small amounts over a period of time[23]. Since malaria parasites actively target RBCs, we explored if healthy RBCs could be preloaded with some of our lead compounds such that these “loaded” RBCs could gain competence to restrict the growth of malaria parasites. Such retention of compounds in RBCs offers a prophylactic strategy that can be useful for passengers prone to traveler’s malaria. Our data showed Bedaquiline as the most promising molecule that is retained by RBCs in a concentration sufficient at preventing the growth of the parasite. Similar but slightly less potent effects were also observed in RBCs preloaded with MMV642550, MMV1634402, and MMV688271.

The finding of potent antiplasmodial activity in Bedaquiline is highly significant since it is a drug already in use against MDR TB[24]. A similar antiplasmodial activity was found in Brilacidin (MMV1634402), a peptidomimetic mimicking the human defensin peptides. Incidentally, Brilacidin has recently been shown to possess antiviral activity against SARS-CoV-2[25] and is currently under human clinical trials for COVID-19 treatment[26]. Our finding of Bedaquiline’s ability to prevent IMC formation and subsequent invasion of merozoites became more interesting when we found that Bedaquiline could cure the mice of malaria infection with mitigation of associated symptoms like pyrexia and weight loss.

As a bonus, we found that combinations of MMV688271, MMV1634402, Hayatinine, Bedaquiline, and Curine with standard antimalarial drugs in specific ratios showed synergistic activity. This seems to open new prospects for use of novel synergistic combinations for the formulation of new ACTs. In conclusion, we have identified GAP50 binder molecules with high selectivity and multistage activity, which can be taken for future drug optimization and development as novel drugs against malaria.

Declarations

Acknowledgment

We are thankful to MMV for providing pathogen and pandemic box compounds. We are grateful to Dr. Pawan Malhotra for providing us with the Phil1 antibody, Dr. Purnima and Swati Gupta for helping with confocal experiments. Thanks to Dr. Arockiasamy Arulandu and Shobhan Kuila for helping with SPR and *in silico* Schrödinger work.

Funding

PA and SK acknowledge the financial support received from the Department of Biotechnology, Government of India and CSIR, New Delhi, respectively, in the form of JRF and SRF fellowship. This work was financially supported by ICGEB, New Delhi.

Disclosure of Interest

The authors declare no competing interests and declare that work done in this manuscript is conceptualized and carried out by PA and DS. Antimalarial activity was evaluated with prior approval (ICGEB/IAEC/30012021/MPB-8) and in accordance with ICGEB animal ethical committee.

Author contribution

PA and DS contributed to the conceptualization of the idea and writing of the manuscript. All experiments and data analysis were done by PA. SK and US provided pure synthetic small molecules and phytometabolites for this work.

References

1. Cowman, A. F. *et al.* Functional analysis of proteins involved in Plasmodium falciparum merozoite invasion of red blood cells. *FEBS Lett.* **476**, 84–88 (2000).

2. Gaskins, E. *et al.* Identification of the membrane receptor of a class XIV myosin in Toxoplasma gondii. *J. Cell Biol.* **165**, (2004).

3. Kortagere, S. *et al.* Structure-based Design of Novel Small-Molecule Inhibitors of Plasmodium falciparum. *J. Chem. Inf. Model.* **50**, 840 (2010).

4. Johnson, S. *et al.* Truncated Latrunculins as Actin Inhibitors Targeting Plasmodium falciparum Motility and Host Cell Invasion. *J. Med. Chem.* **59**, 10994–11005 (2016).

5. Saini, E. *et al.* Photosensitized INA-Labelled protein 1 (PhIL1) is novel component of the inner membrane complex and is required for Plasmodium parasite development. *Sci. Rep.* **7**, 1–11 (2017).

6. SL, F. *et al.* Suramin and suramin analogues inhibit merozoite surface protein-1 secondary processing and erythrocyte invasion by the malaria parasite Plasmodium falciparum. *J. Biol. Chem.* **278**, 47670–47677 (2003).

7. Strath, M., Scott-Finnigan, T., Gardner, M., Williamson, D. & Wilson, I. Antimalarial activity of rifampicin in vitro and in rodent models. *Trans. R. Soc. Trop. Med. Hyg.* **87**, 211–216 (1993).

8. Kimura, A. *et al.* In Vitro and In Vivo antimalarial activities of T-2307, a novel arylamidine. *Antimicrob. Agents Chemother.* **56**, 2191–2193 (2012).

9. Bozdech, Z. *et al.* Expression profiling of the schizont and trophozoite stages of Plasmodium falciparumwith a long-oligonucleotide microarray. *Genome Biol. 2003 42* **4**, 1–15 (2003).

10. Amresh, G., Rao, C. V. & Singh, P. N. Antioxidant activity of Cissampelos pareira on benzo(a)pyrene-induced mucosal injury in mice. *Nutr. Res.* **27**, 625–632 (2007).

11. Yeoman, J. A. *et al.* Tracking glideosome-associated protein 50 reveals the development and organization of the inner membrane complex of Plasmodium falciparum. *Eukaryot. Cell* **10**, 556–564 (2011).

12. Baum, J. *et al.* A conserved molecular motor drives cell invasion and gliding motility across malaria life cycle stages and other apicomplexan parasites. *J. Biol. Chem.* **281**, 5197–5208 (2006).

13. Harding, C. R. *et al.* Gliding Associated Proteins Play Essential Roles during the Formation of the Inner Membrane Complex of Toxoplasma gondii. *PLoS Pathog.* **12**, 1–24 (2016).

14. Saini, E., Kumar, P., Id, S., Id, V. S. & Id, P. A. Plasmodium falciparum PhIL1-associated complex plays an essential role in merozoite reorientation and invasion of host erythrocytes. 1–20 (2021) doi:10.1371/journal.ppat.1009750.

15. The 'World malaria report 2019' at a glance. https://www.who.int/news-room/feature-stories/detail/world-malaria-report-2019.

16. RE, F., G, M. & GH, M. The cytoskeleton and motility in apicomplexan invasion. *Adv. Parasitol.* **56**, 213–263 (2004).

17. AL, B. *et al.* Targeting malaria parasite invasion of red blood cells as an antimalarial strategy. *FEMS Microbiol. Rev.* **43**, 223–238 (2019).

18. Singh, G. P. Conservation of gene essentiality in Apicomplexa and its application for prioritization of anti-malarial drug targets. *F1000Research 2017 623* **6**, 23 (2017).

19. Bosch, J., Paige, M. H., Vaidya, A. B., Bergman, L. W. & Hol, W. G. J. Crystal structure of GAP50, the anchor of the invasion machinery in the inner membrane complex of Plasmodium falciparum. *J. Struct. Biol.* **178**, 61–73 (2012).

20. Beiss, V. *et al.* Plant expression and characterization of the transmission-blocking vaccine candidate PfGAP50. *BMC Biotechnol.* **15**, 108 (2015).

21. Kennedy, A. T. *et al.* Recruitment of Factor H as a Novel Complement Evasion Strategy for Blood-Stage Plasmodium falciparum Infection. *J. Immunol.* 1501581 (2015) doi:10.4049/jimmunol.1501581.

22. Gelb, M. H. Drug discovery for malaria: a very challenging and timely endeavor. *Curr. Opin. Chem. Biol.* **11**, 440–445 (2007).

23. D, S., J, C. & LR, E. Albumin as a versatile platform for drug half-life extension. *Biochim. Biophys. Acta* **1830**, 5526–5534 (2013).

24. Pontali, E., Sotgiu, G., D'Ambrosio, L., Centis, R. & Migliori, G. B. Bedaquiline and multidrug-resistant tuberculosis: a systematic and critical analysis of the evidence. *Eur. Respir. J.* **47**, 394–402 (2016).

25. Bakovic, A. *et al.* Brilacidin Demonstrates Inhibition of SARS-CoV-2 in Cell Culture. *Viruses 2021, Vol. 13, Page 271* **13**, 271 (2021).

26. A Study to Evaluate the Efficacy and Safety of Brilacidin in Hospitalized Participants With COVID-19 - Full Text View - ClinicalTrials.gov. https://clinicaltrials.gov/ct2/show/NCT04784897.

27. Madhavi Sastry, G., Adzhigirey, M., Day, T., Annabhimoju, R. & Sherman, W. Protein and ligand preparation: Parameters, protocols, and influence on virtual screening enrichments. *J. Comput. Aided. Mol. Des.* **27**, 221–234 (2013).

28. Richard A. Friesner, * *et al.* Extra Precision Glide: Docking and Scoring Incorporating a Model of Hydrophobic Enclosure for Protein−Ligand Complexes. *J. Med. Chem.* **49**, 6177–6196 (2006).

29. Paul D. Lyne, *, Michelle L. Lamb, and & Saeh, J. C. Accurate Prediction of the Relative Potencies of Members of a Series of Kinase Inhibitors Using Molecular Docking and MM-GBSA Scoring. *J. Med. Chem.* **49**, 4805–4808 (2006).

30. Bowers, K. J. *et al.* Scalable Algorithms for Molecular Dynamics Simulations on Commodity Clusters. 43–43 (2007) doi:10.1109/SC.2006.54.

31. Kumar, I. *et al.* Photocatalytic Unsymmetrical Coupling of 2-Substituted Quinolines: Synthesis and Evaluation of the Antiplasmodial Potential of β-Norbenzomorphan Frameworks. *ACS Sustain. Chem. Eng.* **8**, 12902–12910 (2020).

32. Bhatt, V. *et al.* Chemical profiling and quantification of potential active constituents responsible for the antiplasmodial activity of Cissampelos pareira. *J. Ethnopharmacol.* **262**, 113185 (2020).

33. Huynh, K. & Partch, C. L. Analysis of protein stability and ligand interactions by thermal shift assay. *Curr. Protoc. protein Sci.* **79**, 28.9.1-28.9.14 (2015).

34. Trager, W. & Jensen, J. B. Human malaria parasites in continuous culture. *Science* **193**, 673–5 (1976).

35. Smilkstein, M., Sriwilaijaroen, N., Kelly, J. X., Wilairat, P. & Riscoe, M. Simple and inexpensive fluorescence-based technique for high-throughput antimalarial drug screening. *Antimicrob. Agents Chemother.* **48**, 1803–6 (2004).

36. Mosmann, T. Rapid colorimetric assay for cellular growth and survival: Application to proliferation and cytotoxicity assays. *J. Immunol. Methods* **65**, 55–63 (1983).

37. Ribaut, C. *et al.* Concentration and purification by magnetic separation of the erythrocytic stages of all human Plasmodium species. *Malar. J.* **7**, 1–5 (2008).

38. Thapar, M. M., Gupta, S., Spindler, C., Wernsdorfer, W. H. & Björkman, A. Pharmacodynamic interactions among atovaquone, proguanil and cycloguanil against Plasmodium falciparum in vitro. *Trans. R. Soc. Trop. Med. Hyg.* **97**, 331–337 (2003).

39. Meletiadis, J., Pournaras, S., Roilides, E. & Walsh, T. J. Defining Fractional Inhibitory Concentration Index Cutoffs for Additive Interactions Based on Self-Drug Additive Combinations, Monte Carlo Simulation Analysis, and In Vitro-In Vivo Correlation Data for Antifungal Drug Combinations against Aspergillus fumigatus. *Antimicrob. Agents Chemother.* **54**, 602 (2010).

40. OECD. Test No. 423: Acute Oral toxicity - Acute Toxic Class Method. *Oecd Guidel. Test. Chem.* 1–14 (2002) doi:10.1787/9789264071001-EN.

41. Ryley, J. F. & Peters, W. The antimalarial activity of some quinolone esters. *Ann. Trop. Med. Parasitol.* **64**, 209–22 (1970).

Methods

Recombinant Expression and affinity purification of *Pf* GAP50

*Pf*3D7 genomic DNA was used to PCR amplify the *Pf*GAP50 gene using *Pf*GAP50 specific primers (5'TTTTCATATGAAATGTCAACTACGCTTTGCG-3'- FP) and (5'-TTTGGATCCTTAATCTTTATTTCCCATGGGTCC-3'- RP). The amplified product was cloned in pET28a$^+$ vector **(SI-1_Fig-7)** which was transformed into Rosetta 2 pLyS strain with ligation of PCR product downstream of His tag sequence. Using 1 % inoculum of the primary culture, secondary culture was initiated in TB broth supplemented with $CoSO_4$ (2 µM), Kanamycin (50 µg/ml), and Chloramphenicol 34 µg/ml[19]. Cells at A_{600} 2.0 were induced with isopropyl β-D thiogalactopyranoside (0.5 mM) at 18 °C for 16 hrs. Harvested cells were lysed by sonication in buffer A (50 mM Tris HCl, pH 8.3 supplemented with 10 % glycerol and 300 mM NaCl). Cellular debris was removed by centrifugation (13000g, 45 min, 4°C) and the clear supernatant was loaded on to a preequilibrated Ni-NTA column. The column was washed using buffer A with 30 column volumes (CV) and the terminal elute was found to be protein-free as tested by Bradford assay. The bound protein was eluted using buffer B (50 mM Tris-HCl, pH 8.3, 500 mM NaCl, 10 % glycerol, 0.5 M imidazole). The eluted proteins were subjected to hydrophobic interaction chromatography by loading them onto a 1M ammonium sulphate in 50 mM Tris-HCl pH 8.3 (Buffer C) preequilibrated phenyl sepharose column followed by washing with buffer C (30 CVs) and elution using 0.4 M ammonium sulphate. The purified protein **(SI-1_Fig-8)** was then dialyzed against the imidazole free buffer B and stored at 4 °C (up to 2 months).

In silico docking, molecular dynamics simulation and -dG of binding

The PDB crystal structure of *Pf*GAP50 (ID: 3TGH) was prepared for docking using the protein preparation wizard[27] of Schrödinger software (version 21-3). Ligand structures drawn using ChemSketch (version 2021.1.2) software were imported into Schrödinger software. Ligprep[27] was used to prepare ligands for docking. Grid was generated to engulf the entire protein, and docking was carried out using the Glide module[28]. Docked poses were then taken for estimation of -dG of binding using the Prime MM-GBSA module[29]. Lead *Pf*GAP50 binders (Bedaquiline, Hayatinine, MMV1634402, MMV688271, and Curine) that showed good promise also in *P. falciparum* culture-based study were taken for the molecular simulation study[30]. Briefly, the protein-ligand complex was solvated using the TIP4PEW model in an orthorhombic box. Na^+ and Cl^- ions were added to neutralize the system. OPLS3e force field was used to simulate for 100 ns. In a quest to determine alternate targets of lead molecules, cross-docking was performed using *in silico* Schrödinger tool. Briefly, malaria parasite protein structures were taken from PDB, and a grid was generated around co-crystallized ligands after preparing the protein and ligand structures. Docking was done using glide module following which binding free energies of protein-ligand complexes were calculated using Prime MM-GBSA tool.

Compounds

Pathogen and Pandemic box compounds dissolved in DMSO at 10 mM were obtained from MMV. Azepino quinolines[31] and molecules from *Cissampelos pareira*[32] (Hayatinine, Curine and Magnocurarine) were from Dr. Upendra Sharma, IHBT, India. The sources of these drug-like molecules were: Bedaquiline (MMV689758) or HY-14881/CS-2921 (Med Chem Express), Mefloquine or M2319 and Bitertanol or 45349 (Sigma), Pentamidine or 20679 (Cayman chemicals), Suramin or 1874-250 (Bio vision), and MMV688771 or S14135SC (May bridge). Additionally, the MMV series of molecules 1634402 (Brilacidin), 1782353, 642550, and 688271 were procured from MMV.

Screening of molecules using differential scanning fluorimetry

Recombinantly expressed and highly purified *Pf*GAP50 was used for *in vitro* small molecule binding using Differential Scanning Fluorimetry (DSF). Compounds were screened at 200 µM using 10 µM of protein. DSF experiment was set up as described by Huynh, K., & Partch, C.L.[33]. T_m was calculated using nonlinear regression model of Boltzmann Sigmoidal curve using the following equation

$$Y = \text{Bottom} + (\text{Top} - \text{Bottom}) / \left\{1 + \exp\left(\text{Tm} - \frac{X}{\text{Slope}}\right)\right\}$$

where Y: fluorescence emission in arbitrary units; X : temperature; Bottom : baseline fluorescence at low temperature; Top : maximal fluorescence; Slope : the steepness of the curve; and T_m :melting temperature of the protein. The binding of some small molecules may manifest as a decrease or increase in protein stability. Molecules that gave a ΔT_m > 2.0 °C over the solvent control were taken as potential hits.

Binding affinity determination using surface plasmon resonance

*Pf*GAP50 (50 µg/ml) was immobilized on a CM5 chip in acetate buffer, pH 4.5 using EDC-NHS coupling. Small test molecules were diluted in 1x PBS supplemented with 5 % DMSO with 0.005 % Polysorbate 20 (running buffer) to yield solutions of varying concentrations (two-fold serial dilution from 50 µM to 0.3125 µM) that were allowed to flow over the immobilized protein at a flow rate of 30 µl/min. Contact and dissociation times of 60 and 120 sec, respectively were given for each cycle. Regeneration was carried out using 10 mM glycine pH 3.0. Data obtained was fitted with a 1:1 binding model to get K_a (association constant), K_d (dissociation constant), and KD (equilibrium binding affinity constant).

In vitro maintenance of *P. falciparum* cultures and assessment of antiplasmodial activity of test molecules

Laboratory adapted *Pf*3D7 (MRA102), *Pf*NDO (MRA819), and *Pf*Cam 3.1^{R539T} (MRA1240) were procured from BEI resources and maintained in O^{+ve} human RBCs collected from Rotary blood bank, New Delhi. Cultures at 4 % haematocrit, (H) were allowed to grow in complete RPMI 1640 medium at 37 $^{\circ}$C under reduced O_2 (gas mixture 5 % O_2, 5 % CO_2, and 90 % N_2) as described by Trager & Jenson[34]. Antiplasmodial activities of test compounds were evaluated by fluorescence-based 96-well format SYBR green I assay as described by Smilkstein et al[35] using chloroquine (4 µM) as zero growth positive control and 0.4 % DMSO as 100 % growth negative control.

In vitro cell cytotoxicity assay against mammalian cell lines

Human cell lines HUH-7 & HEK293 were used to determine cytotoxic effects of test compounds by using MTT [3-(4,5-dimethylthiazol-2-yl)2,5-diphenyltetrazolium bromide] assay for mammalian cell viability as described by Mosmann[36]. Cells were cultured in 10 % fetal bovine serum supplemented DMEM (cDMEM). Briefly, trypsinized cells (10^4 cells/200 µL cDMEM/well) were seeded in triplicate into 96-well flat-bottom tissue-culture plates. Following 16 h cell seeding in triplicate, 200 µL of media was replaced with 96 µL of fresh cDMEM and test molecule solutions (4 µL) were added. Culture plates were incubated for 24 h in a humidified atmosphere at 37 °C and 5 % CO_2. 10 % and 0.8 % DMSO (v/v) were used as +ve (zero growth) and -ve (100% growth) controls respectively. After 24 h treatment, 20 µL MTT (5 mg/mL in 1x PBS) solution was added to each well, and plates were incubated for four hours at 37 °C. Thereafter, plates were centrifuged (700 g, 10 min), and supernatants were aspirated out using a multi pipette. This was followed by the addition of 200 µL of DMSO and incubation of the plate at 37 °C for 10 min. The amount of formazan (a measure of cell growth) formed was assessed by measuring O.D. at 570 nm.

Stage-specific inhibition

*Pf*NDO cultures at 0 to 6 h post-invasion (p.i) (rings), 18 to 22 h p.i (trophozoites), 30 to 34 h p.i (early schizonts), and 40 to 44 h p.i (late schizonts) were incubated with varying concentrations of test molecules for a period of 12 h followed by test molecule removal by centrifugal media washes and allowing cultures to grow for 2nd cycle (48 h) in test molecule free media. IC_{50} (concentration of test molecule at 50 % growth) was obtained by plotting growth curves with untreated, and Chloroquine treated cultures acting as 100 % and 0 % growth controls, respectively.

In vitro test molecule retention by uninfected RBCs

Uninfected RBCs {2 % Hematocrit (H)} were incubated with each test molecule at the respective 10x IC_{50} (*Pf*NDO) for 72 h, followed by three centrifugal washes with 1x PBS. MACS enriched schizonts[37]

{100 % Parasitemia (P)} were added to the washed RBCs at final 1 % P & 2 % H. The plate was then incubated at 37 °C for 96 h with media refreshment every 24 h. Percentage growth was evaluated by SYBR green I lysis method[35], and the cell cycle stage progressions were monitored microscopically using Giemsa-stained smears.

ROS measurement using CM-H2DCFDA dye

ROS measurement was carried out using the protocol provided by the manufacturer (Invitrogen). This technique employs the cell-permeant 2',7'-dichlorodihydrofluorescein diacetate (H_2DCFDA), which in its native ester form is reduced and non-fluorescent. However, inside cells, it is trapped and undergoes esterase catalyzed de-esterification followed by oxidation to the highly fluorescent 2',7'-dichlorofluorescein (DCF). Briefly, *Pf*NDO trophozoites (24 to 28 h p.i) culture at 2 %P and 2 % H was incubated with CM-H_2DCFDA dye (5 µM, 30 min) followed by washing cells with 1x PBS and treatment with test molecules at 2x IC_{50} for 8 h and 12 h respectively. Post-treatment, fluorescence was measured at 530 nm using Spectra Max multi-mode plate reader machine. H_2O_2 (100 µM) treated parasitized RBC (PRBC) and 0.4 % DMSO (v/v) treated uninfected RBC (URBC) were taken as +ve and -ve controls respectively.

Determining stage specificity and kill kinetics of test molecules

To find the stage (s) most vulnerable to the action of test samples, we treated rings (0 to 6 h p.i) with IC_{50} of the test molecules for a maximum period of 57 h allowing ring to ring (RàR) transition with centrifugal wash-based removal of test molecule at hours 12, 24, 36, 48 and 57 of culture. Thereafter, the test molecule-free cultures were allowed to grow under inhibitor-free optimal conditions for a total D^++ D^- time of 96 h. Similarly, to identify schizont inhibitory activity of test molecules, early and late schizonts representing the replicative and invasive phases respectively of the parasite were treated with 2x IC_{50} of test molecules for a total time of 16 h with the removal of test molecules at every 4 h interval followed by culture of the parasite in the absence of test molecules for a total D^++D^- time of 96 h. At the end of the 2^{nd} cycle %, parasitemia was measured by counting 10^5 SYBR green stained cells by FACS.

Egress/invasion inhibition assay

This assay employed a late schizont to early ring (LS à ER) readout where late schizonts were treated with test molecule for 8 h followed by culture in test molecule free medium for a time sufficient to give rings in untreated control culture. For this, *Pf*NDO (42 to 45 h p.i) culture was enriched by the Miltenyi Biotec Magnetic Activated cell sorting (MACS) column[37]. Schizont enriched parasites were diluted to 1

%P at 2 % H in cRPMI and treated with test molecules at 2x IC_{50} for 8 h. This was followed by removal of test molecules by three centrifugal washes with 1x PBS and incubation of the washed cells in fresh cRPMI for 48 h. %P was calculated at the end of the 2^{nd} cycle using SYBR Green staining and counting 10^5 cells via FACS.

Evaluation of GAP50 binder antiplasmodial molecules as disruptors of inner membrane complex formation and invasion

Saini et al[14] have described in malaria parasite the presence of yet another multiprotein complex called Phil1 in close proximity of the glideosomal complex. Interestingly both these complexes present in the space between the plasma membrane and inner membrane have GAP50 as one of the constituents and both complexes appear to play a crucial role in the process of merozoite invasion. In the present work, we have used Phil1 antibodies to track the development of Schizont's inner membrane complex (IMC) in the presence vs absence of the small test molecules that bind GAP50. Early schizonts (30 to 34 h p.i) were treated with test compounds for 12 h, followed by indirect immunofluorescence assay (IFA) to assess IMC development. For this, cells were rinsed once with 1x PBS and fixed using a solution containing paraformaldehyde (4 % v/v) and glutaraldehyde (0.0075 % v/v) in PBS for 30 min. The fixed cells were treated with Triton X-100 (0.1 % v/v) in 1x PBS (twice, 15 min each) and the so permeabilized cells were blocked using BSA (4 % w/v in 1x PBS). Parasites were then incubated with 1°Ab (anti-Phil1, rabbit raised) at 1:50 dilution overnight at 4 °C, followed by washing and incubation with 2 °Ab (Alexa conjugated anti-rabbit antibody 488, Invitrogen) at 1:500 dilution for 3 h at RT. In the end, DAPI (10 µg/mL) was used to stain the nucleus (10 min at RT). Samples were imaged using Nikon A1-R confocal microscope. Similarly, segmented schizont cultures (42 to 46 h. p.i) were treated with test molecules for 8 h and evaluated via IFA for their ability to egress and the resulting merozoites to invade healthy red blood cells leading to the formation of rings.

In vitro potency of the combinations of lead anti-plasmodial molecules

To determine the effect of combining drugs on potency, different drug combinations were made to determine IC_{50} of combinations against synchronous ring stage (6 to 12 h p.i, at 1% P and 2 % H) of *P. falciparum* (MRA1240) in culture. 8x IC_{50} of each test molecule in 10 % DMSO / 1x PBS was taken as stock (A) and mixed with 8x IC_{50} of standard antimalarials (B) in four different molar ratios (4:1, 3:2, 2:3, and 1:4). Each ratio sample was further serially two-fold diluted in 10 % DMSO/ 1x PBS. Four microliters of each dilution were mixed with 96 µl of parasite culture (1% P, 2% H). Thus, each experimental well contained a total volume of 100 µl with or without test molecules. Control (0.4 % DMSO (v/v)) that is nontoxic to the parasite was used as -ve control (100 % growth) whilst Chloroquine (4 µM) was used as + ve control (0 % growth). The plates were incubated (37°C, 72 h) followed by an estimation of parasite

proliferation using the SYBR Green I lysis method[35]. Data analysis was done as described by Thapar et al[38]. The sum of Fractional inhibitory concentrations (∑ FIC) were calculated as FIC_A+FIC_B, where FICs are: FIC_A = IC_{50} of A in combination/IC_{50} of A when alone; FIC_B= IC_{50} of B in combination/ IC_{50} of B alone. The sum of FICs ∑FIC = FIC_A+ FIC_B, was used to classify interactions[39] as synergistic (∑FIC < 1), additive (∑FIC 1.0 - 2.0) or antagonistic (∑FIC > 2.0).

In vivo acute toxicity study

In vivo acute toxicity was done as per OECD 423 guideline[40]. Briefly, mice fasted for 4 h before oral dosing of test molecules. After dosing, mice were kept under observation for the next 45 min for any acute toxicity symptoms followed by resumption of their feed and a daily check over 16 days for any long term toxicity symptoms.

In vivo antimalarial study

In vivo antimalarial study was carried out as per ARRIVE guidelines 2.0 with prior permission from ICGEB animal ethical committee (ICGEB/IAEC/30012021/MPB-8). Briefly, 10^5 *P. berghei ANKA* infected RBCs were injected into mice and grouped randomly with seven mice/group. After 24 h of infection, test molecules were orally administered in vehicle solution (2% (Hydroxypropyl) methylcellulose with 2 % Tween 80 in Normal saline) for four consecutive days followed by daily monitor of %P, body weight, and surface temperature day 5 to day 30[41]. Chloroquine (50 mg/kg b.wt) was taken as + ve control.

Tables

Tables 1-2 are in the supplementary files section.

Figures

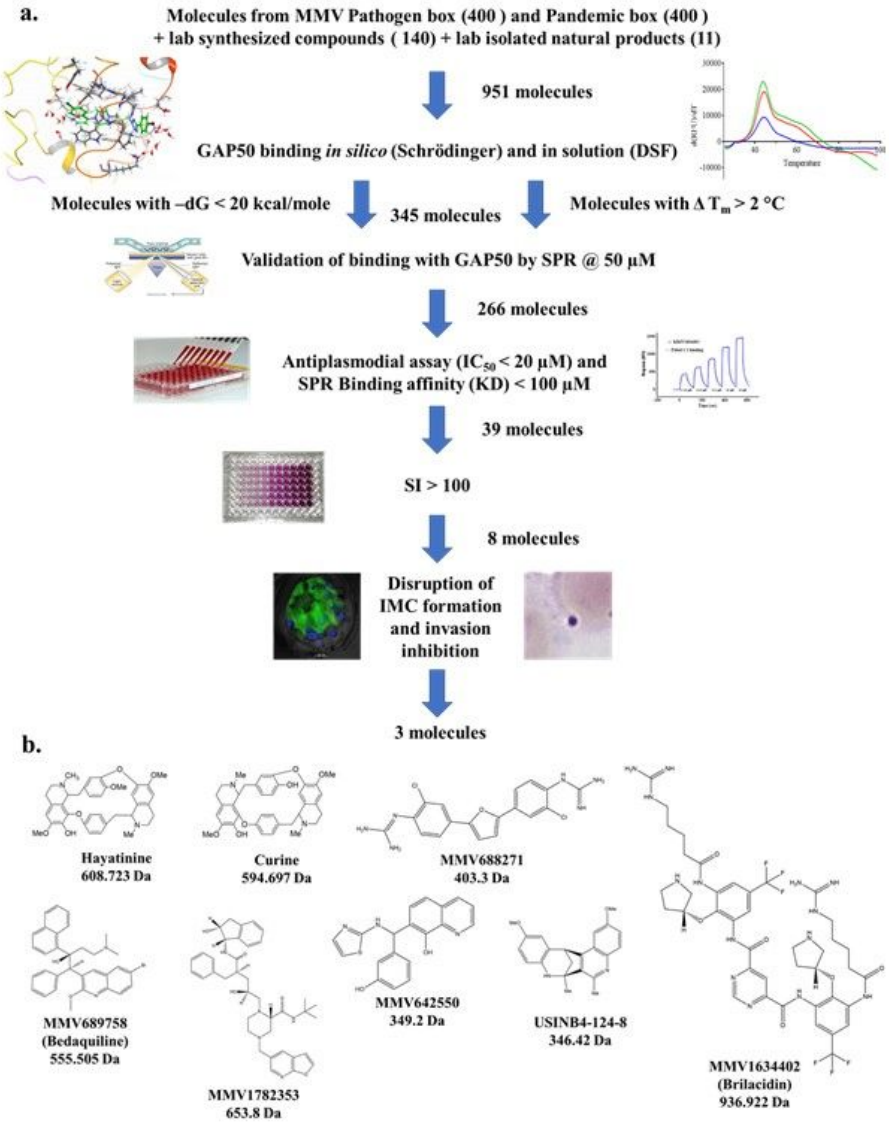

Figure 1: Selection of molecules at successive stages of screenings. (a) Flow chart showing source of the pool of 951 molecules coming from diverse sources and the progressively decreasing numbers of shortlisted molecules at successive stages of different kinds of screens **(b)** Structure of the eight *Pf*GAP50 binder hit molecules with Selectivity Indices ≥ 100. Hayatinine and Curine are isolates from *Cissampelos pareira*, USINB4-124-8 is azepino quinoline, the remaining molecules belonging to MMV pathogen and pandemic boxes were of diverse chemical natures including piperazine carboxamide (MMV1782353), pyrimidine dicarboxamide (MMV1634402), Benzimidazole (MMV642550), quinoline (Bedaquiline), and 2,5-diphenylfuran (MMV688271).

Figure 1

See image for figure caption.

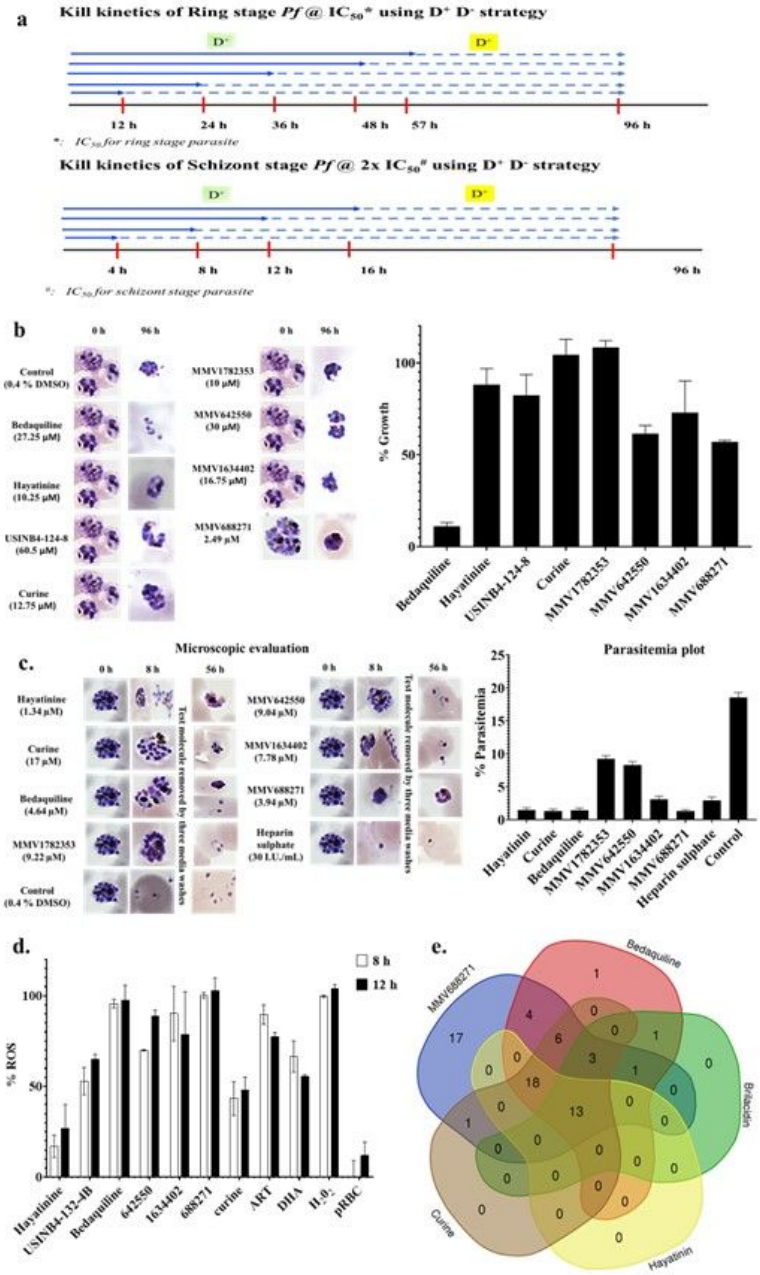

Figure 2: Mechanistic action of GAP50 inhibitors. Pictorial representation of D^+ D^- strategy to study kill kinetics of Ring and schizont stage of *Plasmodium* **(a)**, Effect of preincubation of healthy RBCs with lead antiplasmodial molecules on parasite growth **(b)**, their effect on egress and invasion **(c)** % ROS production **(d)** with **(e)** showing number of common putative target among lead molecule (Hayatinine, Bedaquiline, MMV688271, Brilacidin aka MMV1634402 and Curine) as seen from docking on 68 malaria proteins.

Figure 2

See image for figure caption.

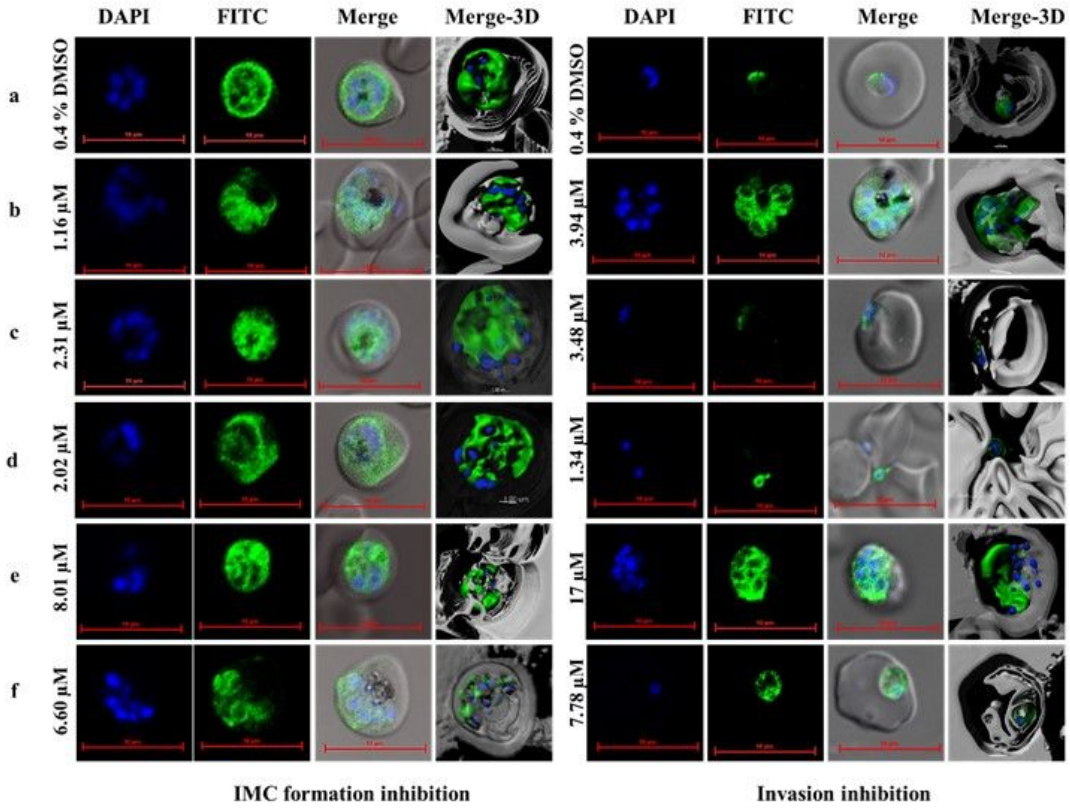

Figure 3: Effect of test molecules on IMC formation (right panel) and invasion inhibition (left panel) using Phil1 as IMC marker. Briefly schizonts (34 to 36 h p.i, right panel) and segmented schizonts (42 to 46 h p.i invasion inhibition column) were treated with test molecules for 12 h and 8 h respectively, followed by confocal imaging to reveal IMC development and invasion inhibition in presence of test molecules. 0.4 % DMSO (v/v) was used as -ve control **(a)**, MMV688271 **(b)**, Bedaquiline **(c)**, Hayatinine **(d)**, Curine **(e)**, and MMV1634402 **(f)**, reflect their effect on IMC formation and invasion inhibition.

Figure 3

See image for figure caption.

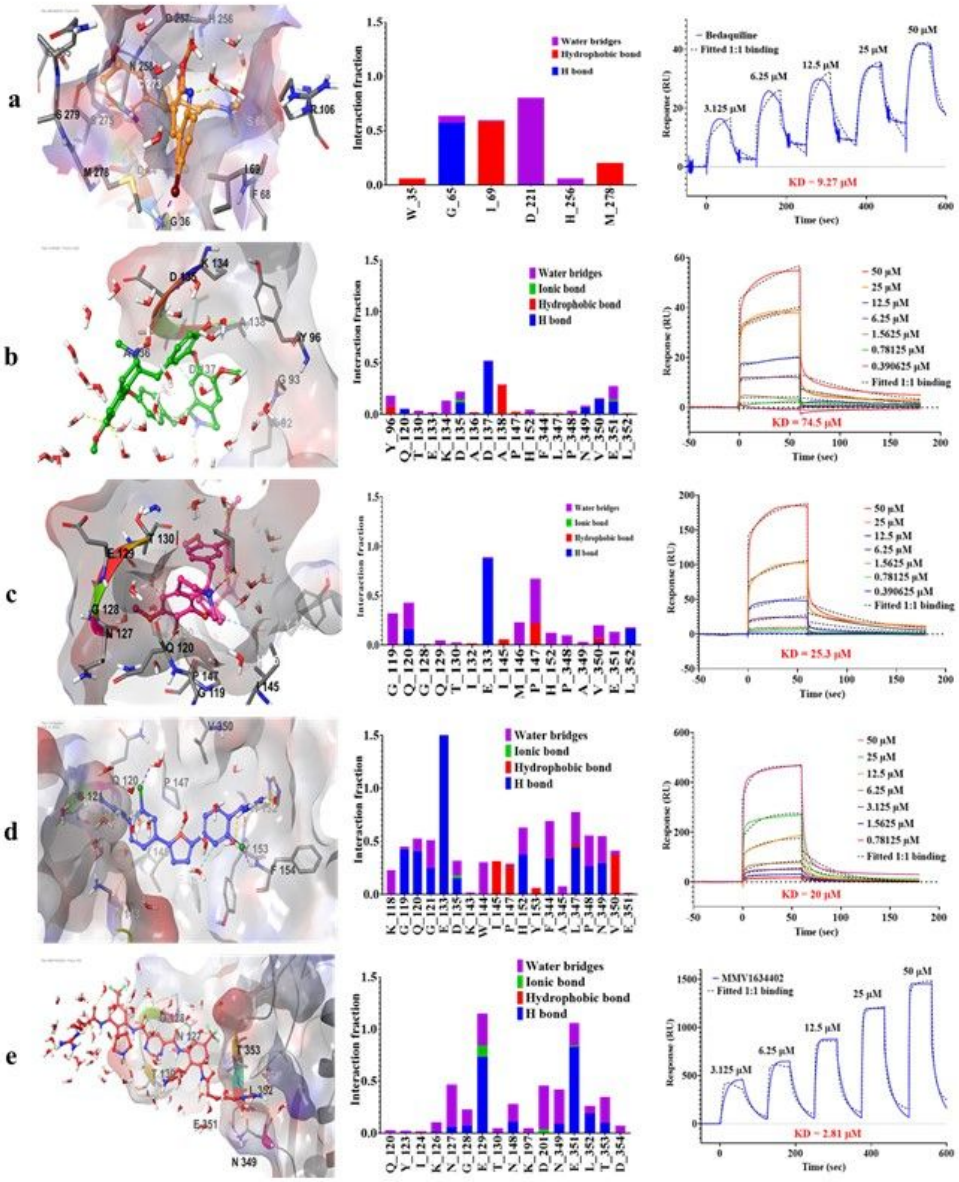

Figure 4: Molecular interaction and SPR kinetics of lead molecules targeting GAP50. Residue wise interactions after MD simulation for 100 nano seconds (left and central panels) and SPR sensorgrams (right panel) are shown for **(a)** Bedaquiline, **(b)** Curine, **(c)** Hayatinine, **(d)** MMV688271 and **(e)** MMV1634402. Ligands are shown in ball and stick representation at the corresponding binding sites on GAP50 represented using electrostatic potential surface map with red and blue colours denoting negative and positive charges, respectively. Nature of interactions of individual amino acid residues are colour coded accordingly.

Figure 4

See image for figure caption.

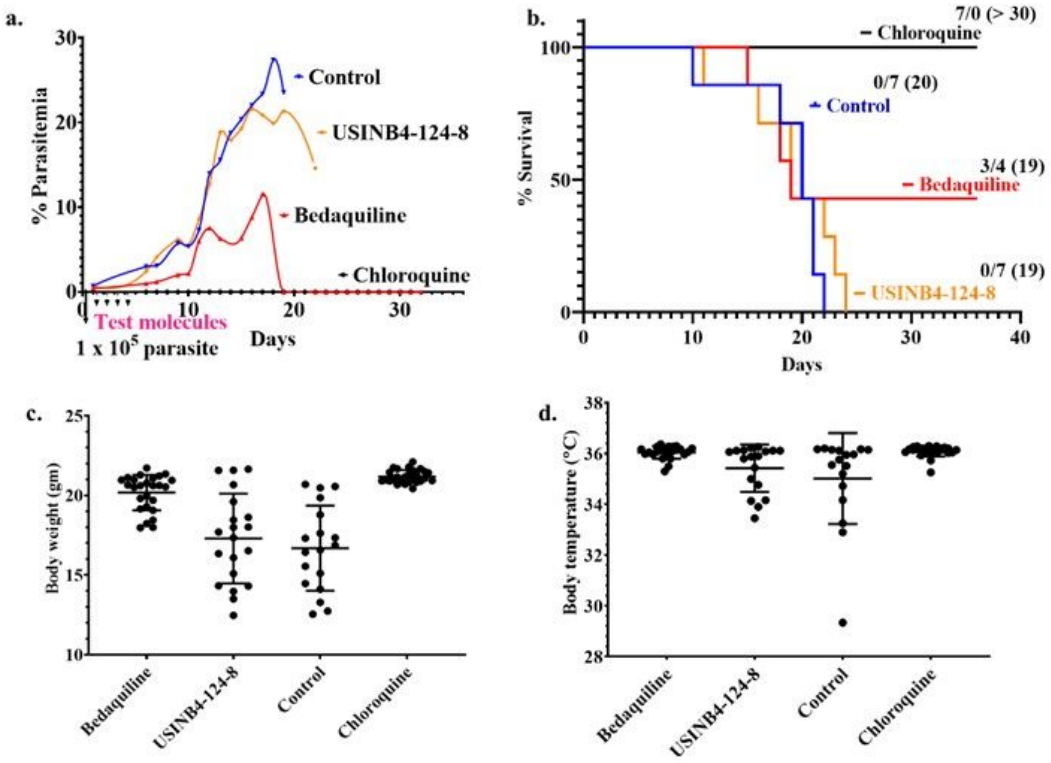

Figure 5: Rise in mean %Parasitemia (a) and median survival time (b) with change in mean body weight (c) and temperature (d). Superscripts in black (B) indicate Alive/Dead mice with mean survival in days in parentheses Each dot in a group (C and D) represents a single day.

Figure 5

See image for figure caption.

Supplementary Files

This is a list of supplementary files associated with this preprint. Click to download.

- Tables.docx
- SI1.docx
- SI2.xlsx